

INTERNATIONAL UNION OF PURE AND APPLIED CHEMISTRY

MACROMOLECULAR DIVISION
COMMISSION ON POLYMER CHARACTERIZATION AND PROPERTIES
WORKING PARTY ON STRUCTURE AND PROPERTIES OF
COMMERCIAL POLYMERS*

STRUCTURE AND MECHANICAL PROPERTIES OF ULTRA-HIGH MOLECULAR WEIGHT POLYETHYLENE DEFORMED NEAR MELTING TEMPERATURE

(Technical Report)

Prepared for publication by

K. NAKAYAMA¹, A. FURUMIYA², T. OKAMOTO², K. YAGI², A. KAITO¹, C. R. CHOE³,
L. WU⁴, G. ZHANG⁴, L. XIU⁴, D. LIU⁴, T. MASUDA⁵, A. NAKAJIMA⁶

¹Research Institute for Polymers and Textiles, 1-1-4 Higashi, Tsukuba, Ibaraki 305, Japan

²Mitsui Petrochemical Co., Ltd., 3-2-5, Kasumigaseki, Chiyoda-ku, Tokyo 100, Japan

³Korea Institute of Science and Technology, P.O. Box 131, Cheongryang, Seoul, Korea

⁴Testing Center of Textile Academy China, P.O. Box 651, Beijing, China

⁵Research Center for Biomedical Engineering, Kyoto University, Kyoto 606, Japan

⁶Osaka Institute of Technology, 5-16-1 Ohmiya, Asahi-ku, Osaka 535, Japan

for the East Asia Sub-Group

Chairman: A. Nakajima; *Secretary:* T. Masuda; *Members:* J. H. Byon; C. R. Choe; T. Hayashi; M. Hirami; M. Isshi; B. Jiang; J. C. Jung; C. K. Kim; C. Y. Kim; K. U. Kim; S. C. Kim; H. Kodama; Y. Kometani; H. Kondo; Y. Kubouchi; J. Li; N. Nagata; K. Nakayama; T. Ohmae; T. Okamoto; R. Qian; K. Sakamoto; S. Shimotsuma; S. Suzuki; S. Tsuchiya; L. Wu; J. K. Yeo; A. Yoshioka

*Membership of the Working Party during the preparation of this report (1987–91) was as follows:

Chairman: 1987–89 H. H. Meyer (FRG); 1989–91 D. R. Moore (UK); *Secretary:* 1987–89 D. R. Moore (UK); 1989–91 M. Laún (FRG); *Members:* G. Ajroldi (Italy); M. Bargain† (France); M. Bevis† (UK); C. B. Bucknall (UK); M. Cakmak† (USA); J. M. Cann (UK); M. J. Cawood† (UK); A. Cervenka (Netherlands); D. Constantin (France); Van Dijk‡ (Netherlands); M. J. Doyle (USA); M. Fleissner (FRG); Franck‡ (FRG); H. G. Fritz (FRG); P. H. Geil (USA); A. Ghijssels (Netherlands); S. K. Goyal† (Canada); D. J. Groves (UK); P. S. Hope (UK); T. A. Huang† (USA); R. J. Koopmans‡ (Netherlands); V. Leo (Belgium); J. Lyngaae-Jorgensen† (Denmark); F. H. J. Maurer† (Netherlands); J. Meissner (Switzerland); H. Motz† (FRG); A. Plochocki (USA); W. Retting (FRG); G. Schorsch‡ (France); H. Schwickert‡ (FRG); H. Schuch† (FRG); J. C. Seferis (USA); S. S. Sternstein (USA); L. A. Utracki (Canada); G. Vassilatos (USA); T. Vu-Khanh† (Canada); J. L. White (USA); C. Wrotecki† (France); H. H. Winter (USA); H. G. Zachmann (FRG).

†1989–91 ‡1987–89

Structure and mechanical properties of ultra-high molecular weight polyethylene deformed near melting temperature

ABSTRACT: Some physical properties of ultra-high molecular weight polyethylene (UHMWPE) were studied in regard to its molecular weight. The main samples employed in this work were three grades of commercially available UHMWPE. UHMWPE is known as a high performance linear polyethylene with excellent physical properties. Owing to its high molecular weight and the presence of entanglements of molecular chains, UHMWPE has very high melt viscosity. The object of this report is to investigate the effect of molecular weight on microstructure and mechanical properties of UHMWPE. Following items are discussed: powder properties of UHMWPE, relationship between properties and molecular weight, and drawabilities at various temperatures. The characteristic features are higher drawability of UHMWPE in the molten state and high tensile moduli of hot drawn sheets. Structure of hot drawn UHMWPE sheets was also discussed.

INTRODUCTION

High density polyethylene (HDPE) is one of the mass production commodity polymers. In general, HDPE is prepared by solution, slurry, and gas-phase polymerization. Slurry polymerization is a widely used method because of possibility of producing wide range of commercial grades including ultra-high molecular weight polyethylene (UHMWPE). UHMWPE is a linear polyethylene with molecular weights over 1×10^6 and is known as a high performance polymer with excellent physical properties, such as high toughness, self-lubrication, and abrasion-resistance. Owing to its high molecular weight and the presence of entanglements of molecular chains, UHMWPE has very high melt viscosity and does not flow like usual polyethylene.

In spite of its poor processibility, UHMWPE is widely used for various applications. Mitsui Petrochemical Industries has been manufacturing UHMWPE. The Sub-Group meeting in East Asia of IUPAC Working Party IV-2-1 has worked to investigate the relationships between molecular weight and physical properties of commercial UHMWPE. This report also describes the drawability of UHMWPE in the molten state and the structure and properties of drawn sheets.

MATERIALS USED AND MOLECULAR CHARACTERISTICS

The samples employed in this report were three grades of ultra-high molecular weight polyethylene (UHMWPE), Hizex Million 145M, 240M, and 340M. Different grades of high-density polyethylene (HDPE) and UHMWPE were also used for comparisons. These polyethylene samples were manufactured by Mitsui Petrochemical Industries. Their molecular characteristics are given in Table 1. Although equations representing the relationship between intrinsic viscosities and molecular weights in the molecular weight region of general-purpose polyethylenes have been proposed by R. Chiang (ref. 1) and P. M. Henry (ref. 2), there is

TABLE 1. Molecular characteristics of polyethylene samples

| Sample | Intrinsic Viscosity $[\eta](\text{dl/g})$ | Molecular Weight $M_v \times 10^{-4}$ |
|--------|---|---------------------------------------|
| PE- 1 | 1.21 | 7.0 |
| PE- 2 | 1.46 | 9.0 |
| PE- 3 | 1.84 | 12.4 |
| PE- 4 | 2.14 | 15.2 |
| PE- 5 | 2.73 | 21.3 |
| PE- 6 | 2.93 | 23.4 |
| PE- 7 | 3.23 | 26.8 |
| PE- 8 | 3.47 | 29.5 |
| PE- 9 | 7.80 | 89.5 |
| PE-10 | 11.3 | 148 |
| PE-11 | 12.2 | 165 |
| PE-12 | 16.8 | 256 |
| PE-13 | 20.7 | 341 |
| PE-14 | 25.6 | 456 |
| PE-15 | 30.5 | 580 |
| PE-16 | 31.4 | 603 |

$[\eta]$: at 135 °C, in decahydronaphthalene

practically no formula proposed for the ultrahigh molecular weight polyethylenes. The only equation ever introduced is the one provided in ASTM D4020 for the relationship between nominal molecular weights and intrinsic viscosities for polyethylenes having reduced viscosities higher than 2.3, which is based on weight average molecular weights. In order to ensure accuracy, it would be more appropriate to discuss the particular relationship in terms of intrinsic viscosities. In our discussion here, however, for the sake of convenience, the molecular weights of all polyethylene samples were converted into the nominal molecular weights, M_v by use of the equation given in ASTM D 4020.

$$M_v = 5.37 \times 10^4 [\eta]^{1.37} \quad (1)$$

The intrinsic viscosities $[\eta]$ were measured in decahydronaphthalene at 135 °C. Commercially available Hizex Million 145M, 240M and 340M correspond to PE-9, PE-12 and PE-14 shown in Table 1, respectively.

POWDER PROPERTIES

UHMWPE is produced by a slurry process and supplied as a fine powder. It is well known that the properties of polymer powder affect the processibility (ref. 3). UHMWPE powders from different suppliers have different powder characteristics (ref. 4). The powder morphologies and thermal properties of the three grades of UHMWPE will be discussed below.

Morphology

The bulk density of three UHMWPE powders was approximately 0.45 g/cm³. The morphology of as-polymerized powder was observed by using a scanning electron microscope (SEM), Hitachi S-800. Fig. 1 shows SEM micrographs of the 240 M powder. The particle diameter is in the order of 200 μm. The secondary particle consists of primary particles. A close observation reveals surface texture of the primary particle.

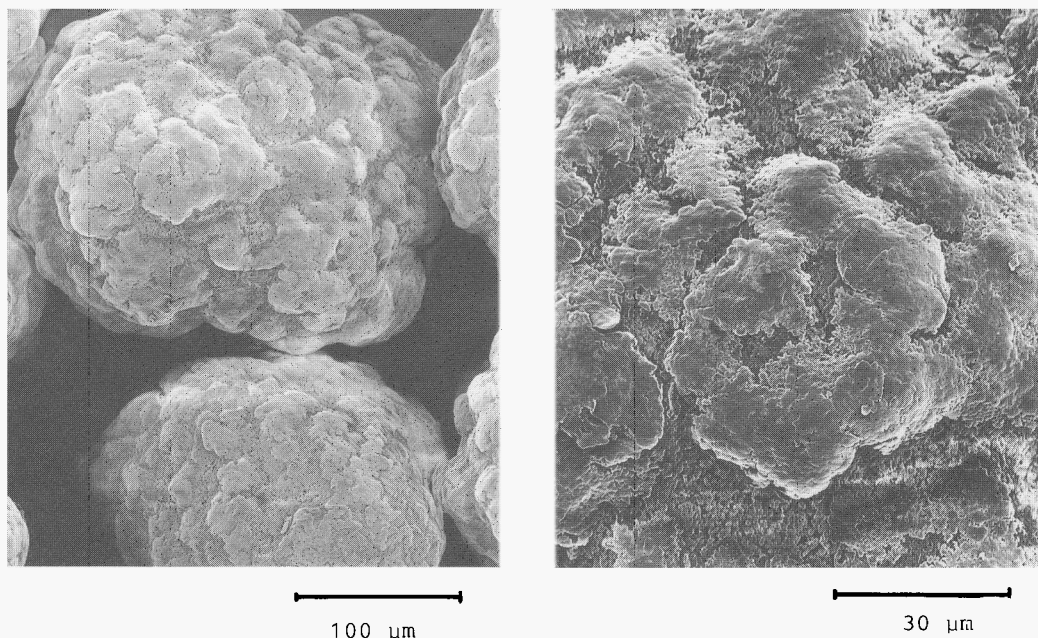


Figure 1. Powder morphology of UHMWPE.

Thermal properties

The melting and crystallization temperatures of powder samples were determined by differential scanning calorimeter (DSC), Seiko DSC 210, calibrated with a melt transition of Indium. Fig. 2 shows the DSC curves of 240 M powder sample. The first and second thermal cycles by heating the sample at a rate of 10 °C/min in nitrogen were recorded. The extrapolated onset, peak and extrapolated end temperatures for melting and crystallization are shown in Table 2. It is seen that the melting temperatures of as-polymerized UHMWPE powders lie in a range of 140 to 143 °C. After the first thermal cycle, the melting temperature decreased by 8 - 10 °C. The peak melting temperature of UHMWPE increases with increasing molecular weight.

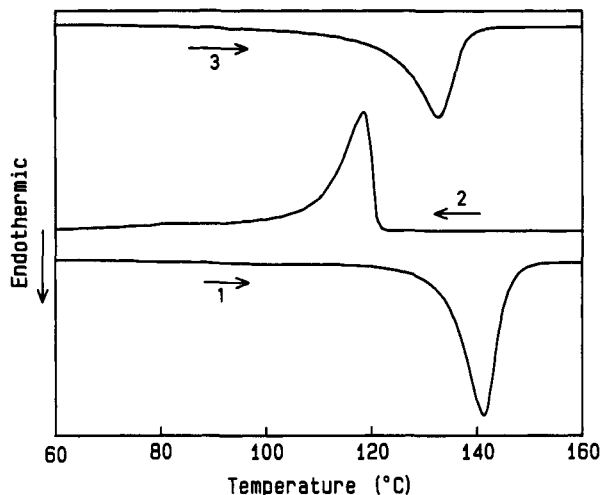


Figure 2. DSC curves for UHMWPE 240 M powder: 1; first heating process, 2; cooling process, 3; second heating process.

TABLE 2. Melting and crystallization temperatures of UHMWPE powder samples

| Powder | First scanning | | | | | | Second scanning | | |
|--------|----------------|----------|----------|----------|----------|----------|-----------------|----------|----------|
| | T_{im} | T_{pm} | T_{em} | T_{ic} | T_{pc} | T_{ec} | T_{im} | T_{pm} | T_{em} |
| 145 M | 130.7 | 140.2 | 147.5 | 118.9 | 116.7 | 107.7 | 121.7 | 132.9 | 139.4 |
| 240 M | 132.8 | 141.2 | 146.3 | 120.6 | 118.2 | 108.2 | 120.6 | 132.9 | 138.1 |
| 340 M | 135.0 | 143.1 | 148.1 | 121.9 | 119.1 | 109.9 | 125.2 | 134.4 | 139.2 |

T_{im} : extrapolated onset temperature of melting
 T_{pm} : melting peak temperature
 T_{em} : extrapolated end temperature of melting
 T_{ic} : extrapolated onset temperature of crystallization
 T_{pc} : crystallization peak temperature
 T_{ec} : extrapolated end temperature of crystallization

PROPERTIES—MOLECULAR WEIGHT RELATIONSHIPS

Chemically, UHMWPE is identical with HDPE. In general, the molecular weight strongly influences on physical properties of polymers. Attempts have been made to deal with the relationships between physical properties and molecular weights of UHMWPE.

Preparation of specimen

The sheets of thickness 1 - 3 mm were prepared by compression molding of UHMWPE powders with a cylindrical type mold. The molding procedures to get homogeneous and uniform specimens are shown in Table 3. The powder was placed in the mold, heated and kept under a pressure of 10 MPa. Pressure applied on the melt was then decreased to 5 MPa. After the dwell-time of 20 minutes, the sample was cooled, kept at 20 - 30 °C under a pressure of 20 MPa and then taken out of the mold.

TABLE 3 Condition for compression molding of UHMWPE

| Step | Temperature (°C) | Pressure (MPa) | Hold time (min) |
|------|------------------|----------------|-----------------|
| 1st | 200 - 220 | 10 | 5 |
| 2nd | 200 - 220 | 5 | 15 |
| 3rd | 20 - 30 | 5 | 0.5 |
| 4th | 20 - 30 | 20 | 20 |

TABLE 4 General properties of polyethylene

| Samples | Molecular Weight $M_v \times 10^{-4}$ | Density $d(\text{g/cm}^3)$ | Vicat softening temperature (°C) | Shore hardness (D scale) |
|---------|--|-------------------------------|-------------------------------------|-----------------------------|
| PE- 1 | 7.0 | 0.962 | 122 | 68 |
| PE- 2 | 9.0 | 0.964 | 124 | 68 |
| PE- 3 | 12.4 | 0.953 | 125 | 64 |
| PE- 4 | 15.2 | 0.956 | 126 | 64 |
| PE- 5 | 21.3 | 0.948 | 120 | 61 |
| PE- 6 | 23.4 | 0.955 | 124 | 64 |
| PE- 7 | 26.8 | 0.955 | 122 | 63 |
| PE- 8 | 29.5 | 0.954 | 126 | 65 |
| PE- 9 | 89.5 | 0.942 | 129 | 65 |
| PE-10 | 148 | 0.947 | 131 | 65 |
| PE-11 | 165 | 0.947 | 130 | 65 |
| PE-12 | 256 | 0.935 | 132 | 63 |
| PE-13 | 341 | 0.938 | 134 | 66 |
| PE-14 | 456 | 0.932 | 134 | 65 |
| PE-15 | 580 | 0.931 | 134 | 65 |
| PE-16 | 603 | 0.931 | 135 | 66 |

General properties

Some physical properties of polyethylene tested are shown in Table 4. The densities of polyethylene sheets are in a range of 0.931 - 0.964 g/cm³ and depend on the molecular weight. In the case of HDPE, with increasing molecular weight, the crystallinity decreases. UHMWPE has relatively low densities.

The softening temperature and hardness are the bases of general properties and important in the end-uses of PE. The Vicat softening temperature is generally used for judging the use-limitations at high temperature. As is understood from Table 4, UHMWPE shows higher heat resistance.

The measurement of Shore hardness was conducted by the use of a type D durometer hardness tester. The scale of hardness was read after the load had been applied on the indenter for 5 s. As shown in Table 4, it is difficult to discuss the exact relationship between the hardness and molecular weight of polyethylene.

The abrasion-resistance of polyethylene sheet was evaluated by the sand abrasion method. Test pieces 75 mm × 25 mm × 6 mm were rotated at 1500 r.p.m. in a sand slurry bath (8 kg of standard sand and 6 kg of water). After the rotation for 20 hrs, the weight loss of specimen sheet was measured. The loss weight is plotted against molecular weight in Fig. 3. Loss weight decreases with increasing molecular weight. The rate of increase of abrasion-resistance with molecular weight is very high at first and finally levels off. The long molecular chain of UHMWPE confers the excellent abrasion-resistance.

Mechanical properties

Mechanical characteristics of polymers are related to molecular weight, crystallinity, orientation, morphological structure and other parameters. Attempts have been made to summarize the mechanical data and correlate mechanical properties to the molecular weight of polyethylene.

The stiffness or relative flexibility of HDPE and UHMWPE was evaluated. The apparent bending modulus of the specimen cut from molded sheet was measured with a cantilever beam testing apparatus, Olsen stiffness tester, in accordance with ASTM D747. The dependence of stiffness on the molecular weight was shown in Fig. 4. Clearly, stiffness decreases with increasing molecular weight.

The long molecular chain of UHMWPE results in high impact toughness. The resistance to breakage by flexural shock of specimen was measured by means of the IZOD and Dynstat tests at room temperature. The effect of molecular weight on the impact strength is shown in Fig. 5. The results of IZOD test are nearly equal to those of Dynstat test. UHMWPE shows an excellent mechanical endurance. An increase in molecular weight is accompanied with an increase in the impact strength and a maximum is exhibited in the region of molecular weight of 1×10^6 and 2×10^6 . In general, an increase in average molecular weight of HDPE leads

to increase in impact strength, but this is achieved when the long-chain molecules are mixed with each other. The impact strength of the UHMWPE of $M_v > 2 \times 10^6$ decreases with increasing molecular weight. This suggests that powder grain boundaries remain in compression molded sheets of higher molecular weight polymer.

The stress-strain measurements were carried out. As shown in Fig. 6, the yield strength of polyethylene decreases monotonically with the molecular weight. The breaking strength rises sharply and polyethylenes of $M_v > 2 \times 10^5$ exhibit higher breaking strengths. When strain at break is plotted against the molecular weight, a maximum appears (Fig. 7). This reduction of elongation at break of higher molecular weight polymers may relate to the powder grain boundaries in compression molded sheets.

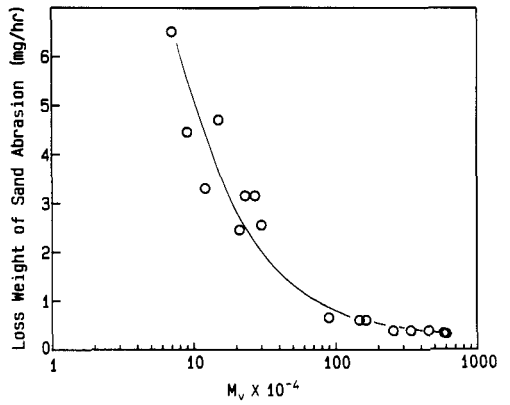


Figure 3. Abrasion-resistance vs. molecular weight for polyethylene samples.

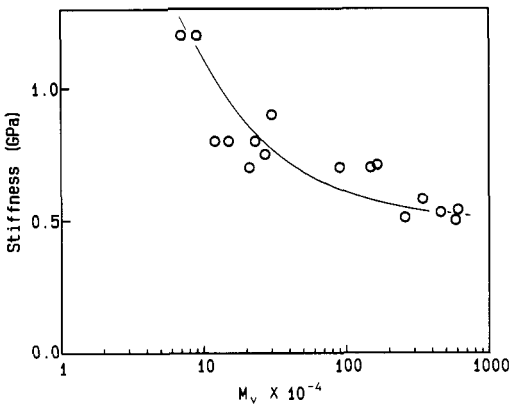


Figure 4. Olsen stiffness vs. molecular weight for polyethylene samples.

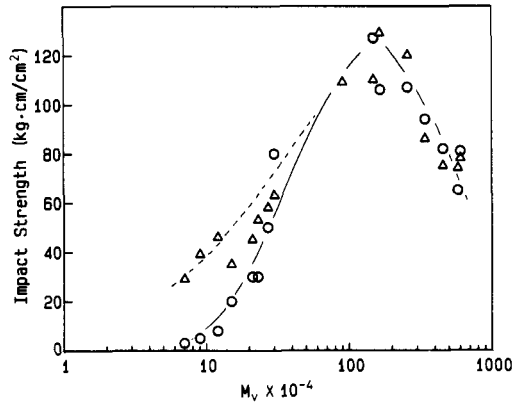


Figure 5. Impact strength vs. molecular weight for polyethylene samples:
 ○; IZOD impact strength,
 △; Dynstat impact strength.

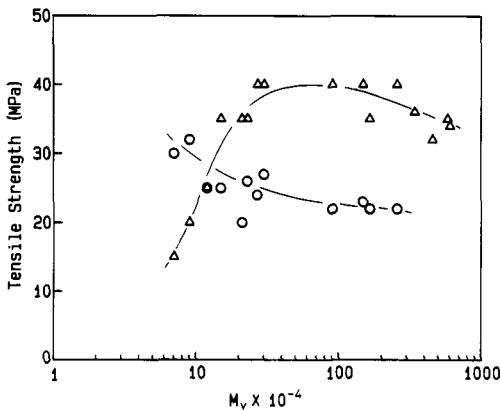


Figure 6. Tensile strength vs. molecular weight for polyethylene samples:
 ○; Yield stress, △; Tensile stress at break.

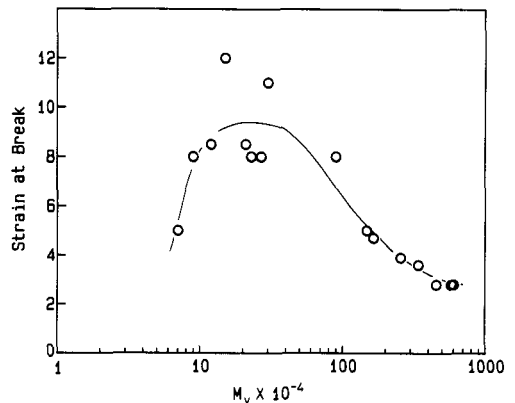


Figure 7. Elongation at break vs. molecular weight for polyethylene samples.

DRAWABILITY OF UHMWPE

The effect of molecular weight on the drawing behavior of linear polyethylene was discussed by Capaccio et al. (ref.5,6) and it was shown that the draw ratio obtainable depended on the molecular weight characteristics of polymer and the crystallization procedures. However, UHMWPE having an excellent physical properties exhibits very high melt viscosity, which may limit its processibility. Here we summarize the drawabilities of three grades of UHMWPE at various temperatures.

Fig. 8 shows the stress - strain curves of 240 M sheet measured at various temperatures for a sample 40 mm in length and at a tensile rate of 50 mm/min. The UHMWPE sheet is able to be stretched even in the molten state. The yield points are observed in the stress - strain curves of melt drawing and solid drawing processes. The strain at yield point for melt drawing is higher than that for solid drawing. The tensile stress for melt drawing is much lower than that for solid drawing.

It is important to consider the presence of a superstructure network formed by entanglement of molecular chains. Owing to the presence of entanglements of molecular chains, the UHMWPE loses fluidity and shows rubber-like elasticity in the melt. In the course of melt drawing, the entanglement plays the role as transmitter of drawing force and the molecular chains supported by the entanglement orient in the stretching direction. This is why the UHMWPE can be stretched in the molten state.

Figs. 9 and 10, respectively, show the temperature dependencies of the initial tensile modulus and of yield stress for UHMWPE. The initial tensile modulus and yield stress gradually decrease with increasing temperature in the solid state and sharply fall off at the melting temperature of UHMWPE. In the solid state, the initial tensile modulus and yield stress are not affected significantly by molecular weight, whereas the tensile properties in the molten state are very sensitive to molecular weight of UHMWPE. As the density of chain entanglements increases with molecular weight, the higher modulus of elasticity is obtained at higher molecular weight in the molten state.

Fig. 11 shows the maximum draw ratio of two grades of UHMWPE as a function of temperature. The maximum draw ratio increases with increasing drawing temperature. The maximum draw ratio for melt drawing is more than twice as large as that for the solid drawing, suggesting that the melt drawing is effective for stretching UHMWPE. At a given temperature, the maximum draw ratio of UHMWPE decreases with increasing molecular weight.

According to the theory of rubber elasticity (ref. 7), the maximum draw ratio of polyethylene is as low as 3.7 (ref. 8), if the entanglements of molecular chains are completely trapped and act as permanent crosslinks during the drawing. As the disentanglement is restricted in lower temperatures, the UHMWPE sheet shows lower extensibility than the normal molecular weight HDPE in the solid state. On the other hand, in the molten state, one can expect the disentanglement of molecular chains through slippage, which makes it possible to stretch the UHMWPE to a higher extension.

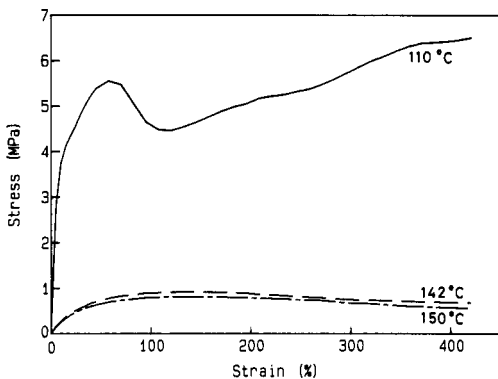


Figure 8. Stress - strain curves at 110, 142, and 150 °C for 240 M sheet.

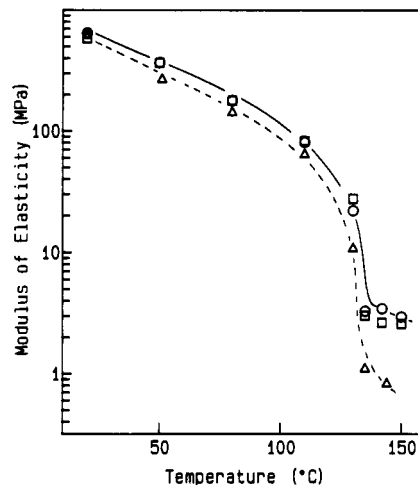


Figure 9. Temperature dependence of initial tensile modulus: Δ ; 145 M, \circ ; 240 M, \square ; 340 M.

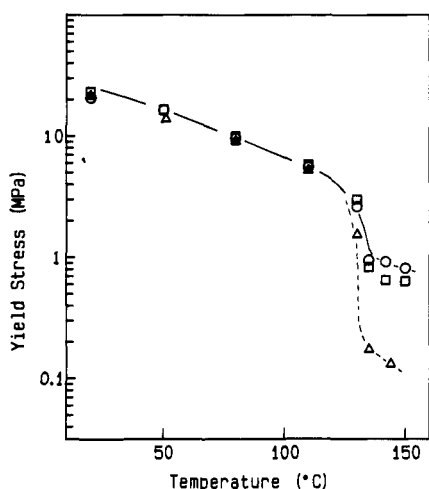


Figure 10. Temperature dependence of yield stress: Δ ; 145 M, \circ ; 240 M, \square ; 340 M

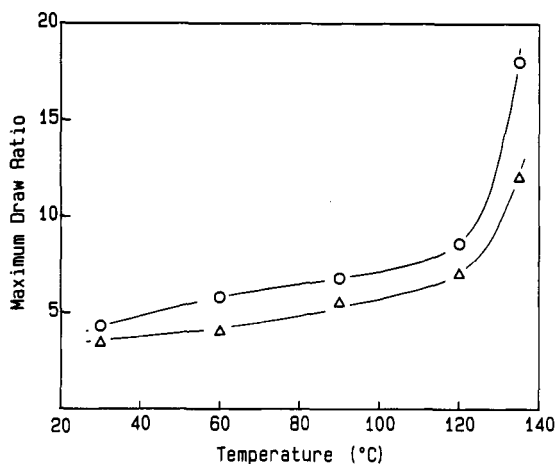


Figure 11. Maximum draw ratio vs. temperature: \circ ; 240 M, Δ ; 340 M

TENSILE PROPERTIES OF HOT DRAWN UHMWPE

Here we summarize the tensile properties of hot drawn UHMWPE sheets. Three grades of UHMWPE samples were used and the uniaxial drawing was conducted in the solid and the molten states. The effects of drawing temperature, drawing ratio, and molecular weight on the tensile properties were investigated.

Strips with gauge dimension of 2×2 cm were uniaxially drawn in the solid state (120-130 °C) and in the molten state (135-150 °C). Tensile properties were measured at 23 °C and a relative humidity of 50 %, with a gauge length of 16 mm and a tensile rate of 4 mm/min.

Figs. 12 and 13 show the Young's modulus and tensile strength, respectively, of hot drawn 145 M sheets. The Young's modulus and tensile strength increase monotonically with increasing draw ratio. The increase of the Young's modulus is quite appreciable in the higher draw ratio range. The Young's modulus and tensile strength are improved more efficiently by solid drawing than by melt drawing. Although the 145 M sheet can be melt drawn at a draw ratio as high as 36 at 135 °C, its Young's modulus and tensile strength are much lower than those obtained by solid drawing.

Figs. 14 and 15 show the Young's modulus and tensile strength, respectively, of the 240 M sheet. The Young's modulus and tensile strength increase with increasing draw ratio analogously to the case of the 145 M sheet. There is however a notable difference between the tensile properties of the melt drawn 145 M and 240 M sheets. Although melt drawing is less effective for increasing the tensile properties of 145 M sheet, the Young's modulus and tensile strength of the 240 M sheet can be much improved by melt drawing. In fact, the Young's modulus of 240 M sheet obtained by melt drawing is higher than that by solid drawing. The tensile strength is more sensitive to drawing temperature than the Young's modulus. At a given draw ratio, the tensile strength of solid drawn 240 M sheet increases with the rise in drawing temperature, while the opposite trend is observed in melt drawn 240 M sheet.

Figs. 16 and 17 show the Young's modulus and tensile strength, respectively, of the 340 M sheet. The tensile properties of hot drawn 340 M sheet show similar tendencies to those of the 240 M sheet in the effects of draw ratio and drawing temperature. However, the maximum draw ratio for 340 M sheet is lower than that for the 240 M sheet. As a result, the highest Young's modulus obtained for 340 M sheet is lower than that of 240 M sheet.

In the course of melt drawing, the entangled molecular chains are aligned in the drawing direction. Accordingly, the tensile properties can be improved by melt drawing. In the case of 145 M with lower molecular weight, the disentanglement takes place more frequently in melt drawing process, which gives negative effect on the transmission of drawing stress and favors the mobility of molecular chains. Therefore, the melt drawing is less effective in the UHMWPE having lower molecular weight.

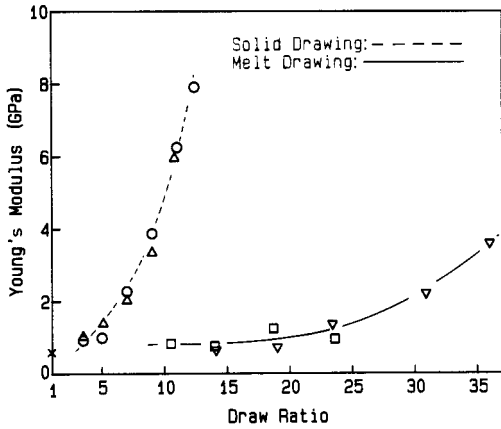


Figure 12. Young's modulus vs. draw ratio for hot drawn 145 M sheets: Δ ; 120 °C, \circ ; 130 °C, ∇ ; 135 °C, \square ; 140 °C

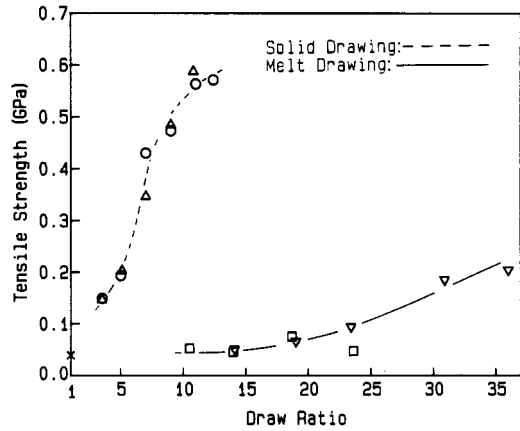


Figure 13. Tensile strength vs. draw ratio for hot drawn 145 M sheets: Δ ; 120 °C, \circ ; 130 °C, ∇ ; 135 °C, \square ; 140 °C

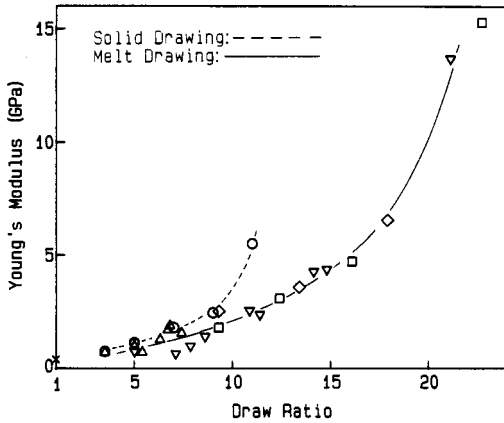


Figure 14. Young's modulus vs. draw ratio for hot drawn 240 M sheets: Δ ; 120 °C, \circ ; 130 °C, ∇ ; 135 °C, \square ; 140 °C, \diamond ; 150 °C.

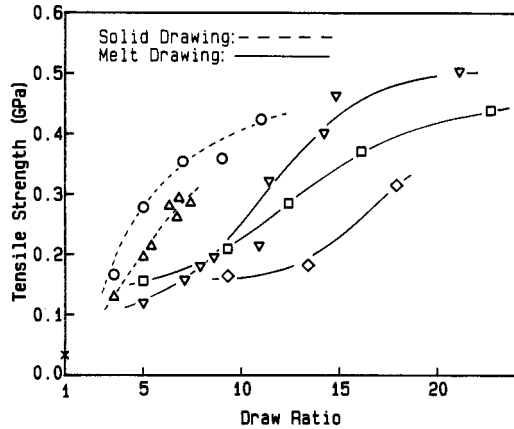


Figure 15. Tensile strength vs. draw ratio for hot drawn 240 M sheets: Δ ; 120 °C, \circ ; 130 °C, ∇ ; 135 °C, \square ; 140 °C, \diamond ; 150 °C.

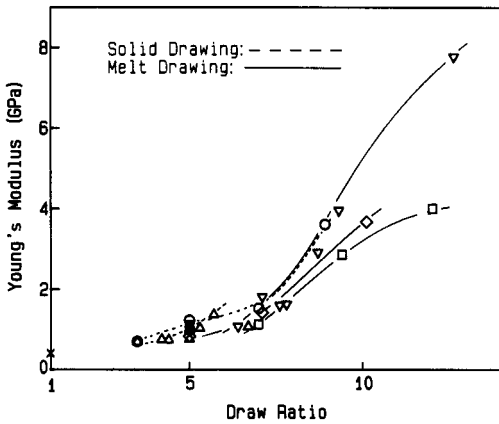


Figure 16. Young's modulus vs. draw ratio for hot drawn 340 M sheets: Δ ; 120 °C, \circ ; 130 °C, ∇ ; 135 °C, \square ; 140 °C, \diamond ; 150 °C.

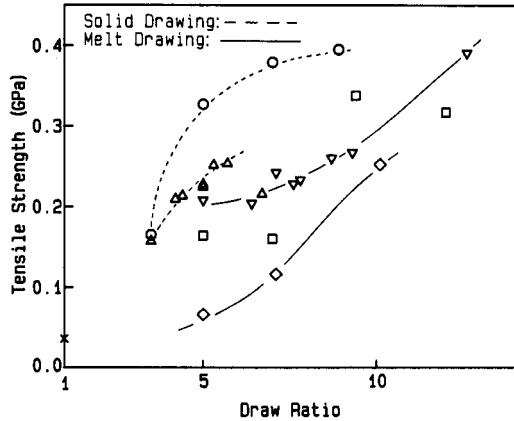


Figure 17. Tensile strength vs. draw ratio for hot drawn 340 M sheets: Δ ; 120 °C, \circ ; 130 °C, ∇ ; 135 °C, \square ; 140 °C, \diamond ; 150 °C.

STRUCTURE OF HOT DRAWN UHMWPE

The structure of hot drawn UHMWPE sheets was characterized by wide angle X-ray diffraction (WAXD), differential scanning calorimetry (DSC), and dynamic mechanical tests. Also, periodic layer structure was investigated by small angle X-ray scattering (SAXS).

The WAXD pole figure was obtained by Ni-filtered Cu K α radiation. The WAXD intensity was measured by employing both Decker transmission method and Schultz reflection method, and then corrected for background and absorption of the specimens. The 200 and 020 pole figures of the melt drawn UHMWPE sheets are shown in Fig. 18. The principal axes of the sheets are labeled M (draw direction), T (transverse direction), and N (normal direction). The 200 and 020 pole densities are distributed in the T - N plane, suggesting that the crystal c-axis orients to the draw direction (M). The b-axis tends to be aligned to the transverse direction, whereas the 200 pole maxima are inclined from the normal direction by 5-15°. The doubly oriented texture might be originated from the kink of crystals.

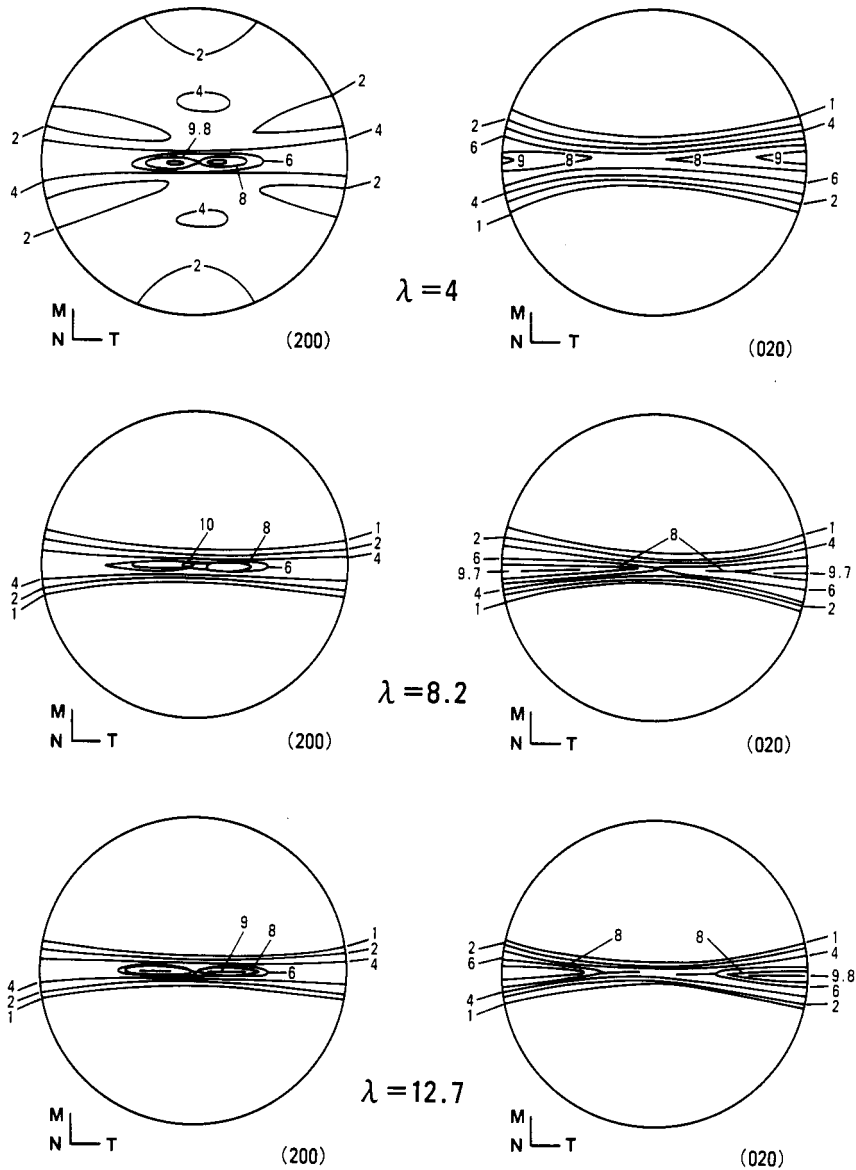


Figure 18. Change of 200 and 020 pole figures of hot drawn 240 M sheets with draw ratios: Drawing temperature; 140 °C.

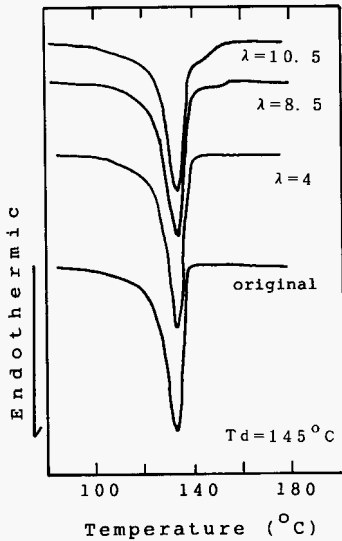
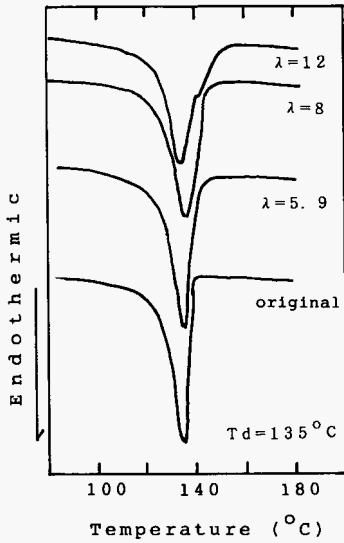


Figure 19. DSC curves of 240 M sheets melt drawn in one stage.

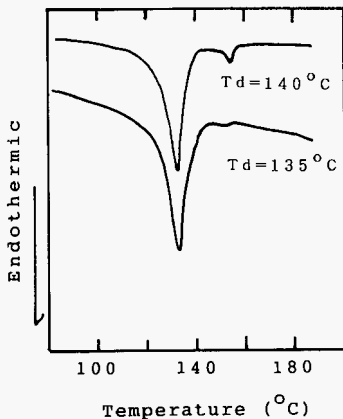


Figure 20. DSC curves of 240 M sheets melt drawn in two stages.

The texture of the sample with lower draw ratio is more complex. The 200 pole figure consists of high maxima on the equator and a small peak at $40 - 45^\circ$ from draw direction to normal direction. The result shows the presence of two modes of orientation of the a-axis: one highly oriented perpendicularly to the draw direction and another weakly oriented between normal direction and draw direction.

The DSC measurements were carried out under a nitrogen atmosphere at a heating rate of 10 K/min. The DSC curves of the melt drawn 240 M sheets are shown in Fig. 19. The temperature at the end of crystal melting shifts to the higher temperature region with increasing draw ratio and a shoulder peak appears on the higher temperature side of the main peak at draw ratios higher than 6. The appearance of the higher melting peak is originated from the extension of molecular chains and the formation of extended chain crystals.

Fig. 20 shows the DSC curves for the 240 M sheets which are melt drawn in two stages. Besides a main peak, a small melting peak is observed at $152 - 153^\circ\text{C}$, suggesting that a small amount of orthorhombic extended chain crystals are produced by the two-stage drawing in the melt state.

Keller et al. proposed a model for the stress-induced crystallization of crosslinked polyethylene (ref. 9,10). The structure development in the melt-drawn UHMWPE sheets can be explained by this model. It is likely that a few extended chain crystals are formed at the initial stage of stretching and act as nucleation centers for the succeeding crystallization process. The crystals grow from the nucleation center, which is aligned to the drawing direction. At high stress (high draw ratio), the crystal grow in a column with the c-axis parallel to the draw direction. On the other hand, at low stress, the crystals grow in the radial direction as in the normal spherulites, without retaining molecular orientation. Both textures are formed at lower draw ratio, giving rise to the bimodal orientation of the a-axis.

The SAXS patterns of the hot drawn sheets were taken with a vacuum camera using a pinhole beam of Ni-filtered $\text{Cu K}\alpha$ radiation. Tsvankin et al. theoretically analyzed the various type of SAXS patterns (ref. 11). Fig. 21 shows the SAXS patterns of the 240 M sheet. The solid drawn sheet shows a four-point pattern which is attributed to a stacking of

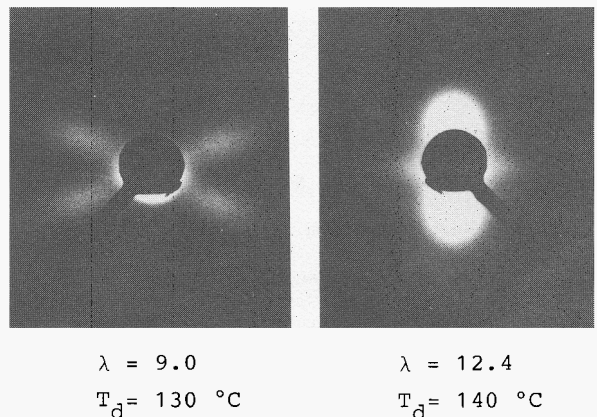


Figure 21. SAXS patterns of 240 M sheets.

inclined periodic layers. The periodic layer is formed by the arrangement of crystallites with the molecular chains parallel to the draw direction. On the other hand, the SAXS pattern of the melt drawn sheet is characterized by a two-point pattern on the meridian. The normals of the periodic layers are aligned parallel to the draw direction in the melt drawn UHMWPE sheet.

The crystallite size along the molecular chain axis (c-axis), D_{002} , was calculated from the broadening of the (002) reflection by using Scherrer's equation. The profiles obtained for the drawn sheets were corrected for instrumental broadening and the $K\alpha$ doublet. Silicon single crystal was used as standard. Crystallite size, D_{002} , long period d , and lattice distortion ϵ , for the drawn sheets of UHMWPE are shown in Table 5. The D_{002} approaches the d in the two-stage drawn sheets. This means that amorphous region between lamellae decreases, and that extended chain crystals are produced and pass through amorphous region. Gibson et al. reported that the crystalline bridges were formed between crystallites in the hot drawn HDPE sheets (ref. 12). As obvious from Table 5, crystallite size along c-axis increases considerably and long period remains fairly constant with increasing draw ratio. Both D_{002} and d decrease in the two-stage drawn sheets. This may be due to smaller draw ratio in the second stage drawing and there are two recrystallization processes: relaxed chains in the melt form folded chain crystals and unrelaxed chains develop extended chain crystals.

Dynamic mechanical behaviors for the drawn sheets reflect also structure characteristics. Fig. 22 indicates that β -relaxation appears in the lower draw ratio sheets. β -relaxation intensity increases due to loosening of network structure formed by entanglement in initial stage of deformation. We suggest that β -relaxation of the drawn sheets of UHMWPE is due to chain segment activities in amorphous region composed of entangled molecules. In higher draw ratio or two-stage drawn sheets, larger size crystals are produced and pass through the amorphous region and thus the amorphous segment activities may decline, so that β -relaxation degenerates greatly or disappears.

REFERENCES

1. R. Chiang, *J. Polym. Sci.*, **36**, 3 (1959).
2. P. M. Henry, *J. Polym. Sci.*, **36**, 91 (1959).
3. R. W. Truss, K. S. Han, J. F. Wallace, and P. H. Geil, *Polym. Eng. Sci.*, **20**, 747 (1980).

TABLE 5. Crystallite size, long period, and lattice distortion of UHMWPE sheets drawn at 140°C

| Draw ratio | D_{002} (Å) | d (Å) | ϵ (%) |
|------------|---------------|---------|----------------|
| 6 | 323 | 414 | 0.36 |
| 8.1 | 355 | 401 | 0.37 |
| 11 | 362 | 410 | 0.11 |
| 22* | 340 | 352 | 0.25 |

*: Two-stage drawing (11 × 2)

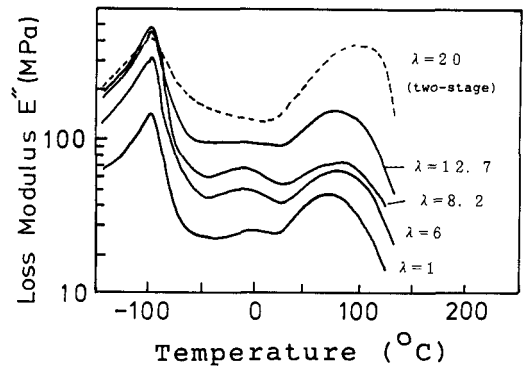


Figure 22. Dynamic mechanical behaviors of UHMWPE sheets drawn at 140 °C: Draw Ratio, A;1, B;6, C;8.2, D;12.7, E;20 (two-stage drawing).

4. G. W. Halldin and I. L. Kamel, *Polym. Eng. Sci.*, **17**, 21 (1977).
5. G. Capaccio and I. M. Ward, *Polymer*, **16**, 239 (1975).
6. G. Capaccio, T. A. Crompton, and I. M. Ward, *J. Polym. Sci., Polym. Phys. Ed.*, **18**, 1301 (1980).
7. L. R. G. Treloar, *The Physics of Rubber Elasticity*, 3rd Ed., Clarendon, Oxford, 1975.
8. P. Smith, P. J. Lemstra, and H. C. Booiij, *J. Polym. Sci., Polym. Phys. Ed.*, **19**, 877 (1981).
9. A. Keller and M. J. Marchin, *J. Macromol. Sci., B*, **1**, 41 (1967).
10. M. J. Hill and A. Keller, *J. Macromol. Sci., B*, **3**, 153 (1969).
11. V. I. Gerasimov, Ya V. Genin, and D. Ya Tsvankin, *J. Polym. Sci., Polym. Phys. Ed.*, **12**, 2035 (1974).
12. A. G. Gibson, G. R. Davies, and I. M. Ward, *Polymer*, **19**, 683 (1978).